

NOTE • OPEN ACCESS

## On fundamental inconsistencies in a commonly used modification of a fluid model for glow discharge

To cite this article: Chen Zhou *et al* 2024 *Plasma Sources Sci. Technol.* **33** 077001

View the [article online](#) for updates and enhancements.

You may also like

- [Liquid metal polymer composites: from printed stretchable circuits to soft actuators](#)  
Carmel Majidi, Kaveh Alizadeh, Yunsik Ohm *et al.*

- [Assessment of weak-coupling approximations on a driven two-level system under dissipation](#)  
W S Teixeira, F L Semião, J Tuorila *et al.*

- [A novel impact identification algorithm based on a linear approximation with maximum entropy](#)  
N Sanchez, V Meruane and A Ortiz-Bernardin

**HIDEN**  
ANALYTICAL

# Analysis Solutions for your **Plasma Research**

**For Surface Science**

- ▶ Surface Analysis
- ▶ SIMS
- ▶ 3D depth Profiling
- ▶ Nanometre depth resolution

**For Plasma Diagnostics**

- ▶ Plasma characterisation
- ▶ Customised systems to suit plasma Configuration
- ▶ Mass and energy analysis of plasma ions
- ▶ Characterisation of neutrals and radicals

Click to view our product catalogue

■ Knowledge  
■ Experience ■ Expertise

Contact Hiden Analytical for further details:  
W [www.HidenAnalytical.com](http://www.HidenAnalytical.com)  
E [info@hiden.co.uk](mailto:info@hiden.co.uk)

## Note

# On fundamental inconsistencies in a commonly used modification of a fluid model for glow discharge

Chen Zhou<sup>1</sup> , Ismail Rafatov<sup>1,2,\*</sup> , Ying Wang<sup>1,3,\*</sup> , Anatoly Kudryavtsev<sup>1,3</sup> ,  
Chengxun Yuan<sup>1,3</sup> , Jingfeng Yao<sup>1,3</sup>  and Zhongxiang Zhou<sup>1,3</sup> 

<sup>1</sup> School of Physics, Harbin Institute of Technology, Harbin 150001, People's Republic of China

<sup>2</sup> Department of Physics, Middle East Technical University, Ankara 06800, Turkey

<sup>3</sup> Heilongjiang Provincial Key Laboratory of Plasma Physics and Application Technology, Harbin 150001, People's Republic of China

E-mail: [rafatov@metu.edu.tr](mailto:rafatov@metu.edu.tr) and [wangying850615@163.com](mailto:wangying850615@163.com)

Received 19 January 2024, revised 18 June 2024

Accepted for publication 3 July 2024

Published 11 July 2024



## Abstract

This work considers the fundamental contradictions in the concept of one of the most well-known and widely used modifications of the fluid model for simulation of a glow discharge (GD), the 'local mean energy approximation' (LMEA). In this model, it is proposed to determine the kinetic coefficients in the electron particle and energy balance equations as functions of the electron mean energy (temperature) rather than local electric field, using a one-to-one correspondence between these parameters through the electron Boltzmann equation. It is shown that the scope of applicability of this model, like any other modification of the fluid model, is limited by the local mode of formation of the electron energy distribution function (EEDF). Therefore, as demonstrated by the examples of typical 1D and 2D problems for a GD in argon, its extension to the region of nonlocal EEDF is in no way justified and leads not only to serious errors in the results, but also to a logically intractable situation in attempts to apply the main postulate of the LMEA model to the region of a weak (or even reverse) electric field in a negative glow plasma. At the same time, the apparent reliability of calculations within the framework of the LMEA model for a number of parameters, in our opinion, only slows down progress in modeling of gas discharge plasma.

Keywords: glow discharge, low-temperature plasma, fluid model, modelling of plasma

\* Authors to whom any correspondence should be addressed.



Original Content from this work may be used under the terms of the [Creative Commons Attribution 4.0 licence](https://creativecommons.org/licenses/by/4.0/). Any further distribution of this work must maintain attribution to the author(s) and the title of the work, journal citation and DOI.

## 1. Introduction

Gas-discharge plasma is a very complex object, the quantitative description of whose properties is possible only by numerical methods. The main reason for this is the need to solve a self-consistent problem taking into account a large number of different kinetic and transport processes, which vary significantly on time, space and energy scales. Therefore, numerical modeling of even such a well-studied plasma object as a DC glow discharge (GD) turns out to be a rather difficult problem. This imposes high demands on numerical models to ensure adequate and accurate descriptions of processes occurring in the plasma.

Methods for numerical simulation of GDs are still under intensive investigation [1–22]. The various approaches that are used to model and simulate GDs can be classified into fluid models, kinetic/particle models and combinations of these, known as hybrid models. The latter represent a compromise between computationally efficient fluid models and fully kinetic/particle models, which require cumbersome computational efforts.

It is commonly accepted that the reliability of a numerical model is determined by its bottleneck, that is, the least accurately known component. Such a component in fluid models of GDs is the description of electron kinetics, because in most cases, the electrons in the plasma of these discharges are far from equilibrium. This is especially the case in the near-cathode regions of GDs, in which the electric field undergoes a sharp change so that the electron energy distribution function (EEDF) and the ionization are of a highly nonlocal nature [23–26]. That means that they are determined not by a local field at a given point in space, but by parameters in the region of the order of the relaxation length of the electron energy relative to a particular collision process of interest.

Recall that GD visually consists of alternating dark and light regions as follows: the dark cathode fall (CF), the negative glow (NG), which is the brightest region of the discharge, the Faraday dark space (FDS), the luminous region of the positive column (PC), and the anode fall region (AF), which is dark in the case of negative anode fall, and bright if the anode fall is positive. Thus, GD contains two primary glowing regions: a PC and a NG. In the plasma of PC, which exists independently of the near-electrode regions of the discharge (NG, FDS, and AF), excitation and ionization are caused by a local electric field. This is why models based on the so called local field approximation (LFA), in which the electron kinetic coefficients are defined as functions of the local value of the reduced electric field  $E/N$  (where  $E$  is the magnitude of the electric field and  $N$  is the background gas density), describe the PC satisfactory well.

On the contrary, plasma of the NG with a weak (and even reverse) electric field is formed by the ‘external’ ionizing factor, namely, an electron beam emitted from the CF. The transition from the NG to the luminous PC always occurs through the formation of a dark FDS region. However, the formation of the dark region of the FDS between the luminous regions of the NG and PC in the conducting plasma channel is

completely impossible to explain within the framework of traditional concepts based on the local field. Therefore, such self-organization of a GD cannot be described within the framework of the LFA; it can only be understood on the basis of nonlocal electron kinetics [23–26].

To extend the fluid model to describe the entire GD, a modification was proposed in [9, 27], which is sometimes referred to as the ‘extended fluid model’ [4] or the ‘local mean energy approximation’ (LMEA) [28]. Within this model, the local dependence of the electron induced elementary processes on the electric field is replaced with a dependence on the electron temperature. In fact, this approach employs a one-to-one correspondence between the electric field  $E/N$  and electron temperature  $T_e$  (defined as two-thirds of the mean electron energy), through the solution of the local kinetic Boltzmann equation with corresponding cross-sections (for details, see [4, 6, 7, 9, 28]). Indeed, as it can be seen from figure 1, temperature  $T_e$  is monotonically increasing function of  $E/N$ . Due to this correspondence, electron kinetic coefficients (electron transport coefficients as well as rate constants of electron-induced plasma-chemical reactions) can be tabulated (‘look-up-tables’, LUTs) as functions of the electron temperature,  $T_e$ , rather than the local value of the electric field  $E/N$ . Within this approach, the electron temperature is obtained from the energy balance equation, in which, along with the processes of heating (or cooling) of electrons, the spatial transfer of electron energy due to thermal conductivity is also taken into account. Consequently, the electron temperature, as well as other electron characteristics (such as rate constants of electron impact reactions), are no longer determined by the local value of the electric field at a given point in space, but in a region of the order of the electron thermal conductivity length

$$\lambda_T = \lambda/\sqrt{\delta} \gg 100\delta, \quad (1)$$

where  $\lambda$  is mean free path of electrons and  $\delta = m_e/M$  is the energy exchange factor. A strong flow of electron heat from the cathode layer results in a rather large  $T_e$  in the plasma of NG. Electrons at these temperatures provide an ionization rate sufficient to maintain the discharge even in the absence of an electric field (or even with an reverse electric field cooling the electron gas).

Recently, the LMEA model has been included in commercial computational software packages [29, 30], which have convenient, user-friendly interfaces for operation, and supplied with extensive databases, detailed manuals, and application libraries with typical test problems for modeling various types of gas discharges. Taking into account the ability of the LMEA model to simulate the entire gas-discharge gap (‘from the cathode to the anode’), all this made it possible for a wide range of users to carry out modeling in a variety of scientific and applied research. This led to an explosion of publications on modeling various gas-discharge devices. However, neither the applicability criteria nor the fundamental contradictions and limitations existing in the concept of this method [23–26] are indicated in the corresponding manuals and tutorials. As

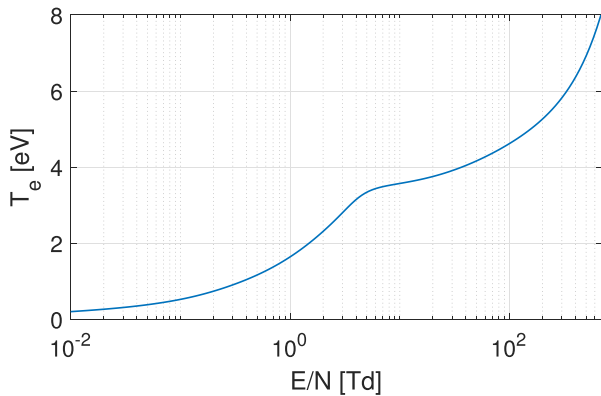


**Figure 1.** Relationship between electron temperature and electric field derived from the local Boltzmann equation. Calculations were done for argon gas.

a result, inexperienced novice researchers (especially, undergraduate and graduate students) have a false impression of the universality of the LMEA model and the possibility of its use without restrictions for modeling various types of gas discharges, presented in manuals and tutorials as test problems.

However, in the LMEA model, as in any other type of fluid model, the derivation of the basic equations is based on the assumption that the EEDF is factorized as a product (see (8) in [9])

$$f_0(\varepsilon, \mathbf{r}, t) = n_e(\mathbf{r}, t) F_0(\varepsilon). \quad (2)$$

Here, the electron density  $n_e(\mathbf{r}, t)$  is a function of spatial coordinates and time, the EEDF itself  $F_0(\varepsilon)$  is a function of the electron kinetic energy  $\varepsilon$ , and depends also on the local electric field  $E/N$  and other parameters (such as the gas temperature, density of excited particles, etc) in the given point of space  $\mathbf{r}$ .

Therefore, factorization (2) assumes the existence of a local EEDF at each point in space. This makes it possible to describe the entire electron ensemble by means of an ‘average’ electron, characterized by a common average directional velocity and average energy (temperature). In this formulation, to describe the properties of the entire ensemble of electrons, it is sufficient to multiply these characteristics by the corresponding particle density. However, on scales smaller or of the order of  $\lambda_T$ , electrons of different energies (belonging to different parts of the EEDF) have different times and lengths of their energy relaxation and behave independently of each other (they do not have time to ‘mix’ due to collisions in the volume and to form a single local EEDF) (for details, see [23–26]). Therefore, the LMEA model, as well as its main postulate about the one-to-one correspondence between the electric field and electron temperature, are applicable only under conditions when the spatial size of the plasma is greater than the energy relaxation length of electrons (1), and the ambipolar field is small compared to the heating field, which is responsible for the production of charged particles by electron impact ionization [31, 32].

Since modeling using a commercial computational package (such as COMSOL Multiphysics with Plasma Module)

implies a computational domain occupying an entire interelectrode space, the modeling results inevitably include near-electrode and near-wall plasma regions. At the same time, spatial dimensions within which the LMEA model is *a priori* inapplicable, are quite large and exceed the electron mean free path by two orders of magnitude (see (1)). It should be mentioned that DC hollow cathode discharges, low pressure CCP discharges, etc consist exclusively of layers of space charge and negative-glow plasma with a weak (or reverse) field, formed by nonlocal ionization by fast electrons that have gained their energy in the strong field of the space charge. Since the characteristic sizes of these discharges are smaller than the energy relaxation length of electrons, the LMEA model is obviously inapplicable for describing such discharges.

Unfortunately, the fundamental work on the LMEA model [9] does not present or discuss in any way the conditions under which factorization (2) of the EEDF is valid. Moreover, in the specialized literature, due attention is not paid to the criteria for the applicability of the LMEA model. For a specialist in electron kinetics, this issue may be clear already from derivation of the fluid equations system, and from his standpoint, explicit formulation of the applicability criteria may not be necessary. However, for a large number of novice users of commercial computational packages, the lack of these criteria in the corresponding manuals and tutorials involuntarily assumes the universality of using the LMEA model for modeling various gas discharges described in these software packages.

The extension of the LMEA model to the region of nonlocal EEDF is in no way justified and, as shown in this work, leads not only to serious errors in the results, but also to a logically intractable situation in attempts to apply the main postulate of the LMEA model (depicted in figure 1) to the region of the reverse electric field in plasma of NG. Consequently, the qualitative plausibility of some discharge parameters calculated from the LMEA model, in our opinion, hardly encourages progress in modeling of gas discharge plasma. These facts raise doubts about the adequacy of the LMEA model to the real situation. This paper is intended to draw attention to this problem.

Section 2 provides a summary of commonly used GD modeling techniques. In section 3, the inconsistency within the LMEA is identified and illustrated using typical 1D and 2D problems for a GD. This section also illustrates performance of different modeling techniques on the example of 1D problem for a GD. The paper concludes with section 4.

## 2. Commonly used methods for GD simulations

### 2.1. Fluid models

The fluid model with its various modifications is the most commonly used method for numerical modeling of gas discharges. Fluid equations of GDs are usually reduced to drift–diffusion equations for charged and neutral plasma species,

**Table 1.** Boundary conditions on the cathode and anode used in the model.

Species type	Cathode ( $z = 0$ )	Anode ( $z = L$ ) and dielectric wall ( $r = R$ )
Electrons	$\hat{\mathbf{n}} \cdot \mathbf{\Gamma}_e = \frac{1}{4} v_e n_e - \gamma \hat{\mathbf{n}} \cdot \mathbf{\Gamma}_i$	$\hat{\mathbf{n}} \cdot \mathbf{\Gamma}_e = \frac{1}{4} v_e n_e$
Ions	$\hat{\mathbf{n}} \cdot \mathbf{\Gamma}_i = \frac{1}{4} v_i n_i + a n_i \mu_i (\hat{\mathbf{n}} \cdot \mathbf{E})$	$\hat{\mathbf{n}} \cdot \mathbf{\Gamma}_i = \frac{1}{4} v_i n_i + a n_i \mu_i (\hat{\mathbf{n}} \cdot \mathbf{E})$
Metastable atoms	$\hat{\mathbf{n}} \cdot \mathbf{\Gamma}_m = \frac{1}{4} v_m n_m$	$\hat{\mathbf{n}} \cdot \mathbf{\Gamma}_m = \frac{1}{4} v_m n_m$
Electron energy density	$\hat{\mathbf{n}} \cdot \mathbf{\Gamma}_\varepsilon = \frac{1}{3} v_e n_\varepsilon - 2k_B T_e \gamma \hat{\mathbf{n}} \cdot \mathbf{\Gamma}_i$	$\hat{\mathbf{n}} \cdot \mathbf{\Gamma}_\varepsilon = \frac{1}{3} v_e n_\varepsilon$
Electric potential	$\varphi = 0$	$\varphi = U_d (z = L)$ and $\hat{\mathbf{n}} \cdot \nabla \varphi = \frac{1}{\varepsilon_0} \sigma (r = R)$

$$\frac{\partial n_k}{\partial t} + \nabla \cdot \mathbf{\Gamma}_k = S_k, \quad (3)$$

with particle fluxes  $\mathbf{\Gamma}_k$  expressed in the form

$$\mathbf{\Gamma}_k = \text{sgn}(q_k) n_k \mu_k \mathbf{E} - D_k \nabla n_k. \quad (4)$$

These equations are coupled to the Poisson equation for the electrostatic potential  $\varphi$

$$\epsilon_0 \nabla \cdot \mathbf{E} = \sum_k q_k n_k, \quad \mathbf{E} = -\nabla \varphi. \quad (5)$$

In these equations, subscript  $k$  indicates the  $k$ th species (we also use subscripts  $i$ ,  $e$ ,  $m$  and  $g$  to specify ions, electrons, metastable atoms and background gas, respectively),  $S$  denotes the particle creation/destruction rate,  $\mathbf{E}$  is the electric field,  $q$  is the charge,  $\epsilon_0$  is the dielectric constant,  $\mu$  and  $D$  denote the mobility and diffusion coefficients. The effect of particle collisions is taken into account by the transport (mobility and diffusion) and reaction rate coefficients.

In the case of the model based on the LFA, the ionization is usually determined using the Townsend formula  $S_e = S_i = |\mathbf{\Gamma}_e| A p \exp(Bp/|\mathbf{E}|)$ , where  $A$  and  $B$  are the constant parameters defined by the type of gas [33]. As we already mentioned in the previous section, in the near-cathode region of a GD, the ionization is not determined by the local field and, therefore, the LFA-based models are inapplicable [23, 24].

A modification of the fluid model, intended to overcome the shortcomings of the LFA by including the spatial transfer of electron heat into the model, was proposed in [27]. It is known in the literature as the ‘extended fluid model’ or ‘local mean energy approximation’ (LMEA) as opposed to the ‘local field approximation’ (LFA). Within this model, the coefficients of the elementary processes involving electrons (electron mobility and diffusion coefficients  $\mu_e$  and  $D_e$ , as well as rate constants of the electron-induced reactions) are calculated by convolving the EEDF, obtained from the solution of the local Boltzmann kinetic equation, with the corresponding cross-sections (we used the BOLSIG+ solver in this work, for details, see [9]). These data are tabulated as functions of the electron temperature  $T_e$  rather than the local electric field  $E$ , and incorporated into fluid model, to solve the electron particle and energy balance equations.

Within LMEA, the system of particle balance and Poisson equations (3)–(5) is supplied by the electron energy balance equation,

$$\frac{\partial n_\varepsilon}{\partial t} + \nabla \cdot \mathbf{\Gamma}_\varepsilon = S_\varepsilon, \quad (6)$$

with the density of the electron energy flux of the form

$$\mathbf{\Gamma}_\varepsilon = -D_\varepsilon \nabla n_\varepsilon - \mu_\varepsilon \mathbf{E} n_\varepsilon. \quad (7)$$

This allows to specify the electron temperature,  $T_e$ , through the relation between the electron energy density,  $n_\varepsilon = n_e \bar{\varepsilon}$ , and the mean electron energy,  $\bar{\varepsilon} = 3/2 k_B T_e$ . The energy transport coefficients are related to particle transport coefficients via  $\mu_\varepsilon = (5/3) \mu_e$  and  $D_\varepsilon = (5/3) D_e$  [9]. Source function in this equation  $S_\varepsilon = P_{\text{heat}} + P_{\text{el.}} + P_{\text{inel.}}$  includes the Joule heating (or cooling) of electrons in the electric field,  $J_{\text{heat}} = -e \mathbf{\Gamma}_e \cdot \mathbf{E}$ , the elastic losses,  $P_{\text{el.}} = -\frac{3}{2} \delta \nu_{ea} n_e k_B (T_e - T_g)$ , and the energy loss in inelastic collisions,  $P_{\text{inel.}} = -\sum_j \Delta E_j R_j$ . In these equations,  $\nu_{ea}$  denotes the electron-atomic elastic collision frequency,  $k_B$  is the Boltzmann constant,  $\delta = 2m_e/m_g$ ,  $m$  is the particle mass,  $T_g$  is the background gas temperature,  $\Delta E_j$  and  $R_j$  are the energy loss (or gain) due to inelastic collision and corresponding reaction rate.

The boundary conditions are specified in table 1 [34]. There,  $v_j = \sqrt{8k_B T_j \pi m_j}$  ( $j = e, i, m$ ) denotes the thermal velocity, the flux density  $\mathbf{\Gamma}$  is described by the equations (4) and (7),  $\hat{\mathbf{n}}$  is the normal unit vector pointing towards the surface, and  $\alpha$  is a switching function (either 0 or 1) depending on positive ion drift direction at the surface:  $\alpha = 1$  if  $(\hat{\mathbf{n}} \cdot \mathbf{E}) > 0$ , and  $\alpha = 0$  otherwise,  $\gamma$  is the secondary electron emission coefficient. The surface charge density  $\sigma$  is calculated from the equation  $\partial \sigma / \partial t = \hat{\mathbf{n}} \cdot e (\mathbf{\Gamma}_i - \mathbf{\Gamma}_e)$ .

## 2.2. Kinetic models

Within the framework of the kinetic model [11, 35–37], ions and metastable atoms are described by fluid equations, while the electronic characteristics are determined by numerically solving the nonlocal (spatially non-homogeneous) Boltzmann equation. In fact, the most accurate description of the electron behavior in plasma of gas discharges is obtained from models of this type. However, this approach is very complicated both in terms of implementation and computational resources, especially if more than one dimension needs to be taken into consideration.

The method known as PIC/MCC (Particle in cell/Monte Carlo collision) is also classified as belonging to the kinetic methods. It combines Monte Carlo simulations of electron and ion dynamics with Poisson’s equation for a self-consistent electric field. It is also computationally expensive, and is not widely used in gas discharge modeling [2, 5, 13, 38–42]. Indeed, this approach requires enormous computational efforts, because a reasonably large number of superparticles must be involved in the simulations to obtain accurate and

noise-free results. It is important to note that the low reliability of cross-section data for plasma processes, especially the angular dependence of scattering, limits the accuracy of such detailed, direct-method computations. It should be also pointed out that this method is hardly suitable for DC discharges. This issue was reported earlier in the literature [6]. Indeed, using our PIC/MCC numerical code [42] we were unable to obtain a convergent solution in an acceptable time.

### 2.3. Hybrid models

Hybrid models, in which slow plasma species are incorporated within the frame of the fluid model, while fast species (particularly fast electrons, using Monte Carlo simulations) are treated as particles, provide another way to address the shortcomings of the fluid model [6, 43–47].

## 3. Results and discussions

### 3.1. 1D example

At the first stage, we consider 1D model of a short (without PC) GD, the computational characteristics of which are the simplest to analyze and interpret because its plasma region consists of only one NG. We assume that the discharge is maintained in argon at a pressure of  $p = 1$  Torr, the gas gap is  $L = 1$  cm. For the short GD under consideration, the literature contains simulation results obtained by various authors for different models listed in section 2. Moreover, reliable analytical models and scalings have also been developed [23, 24], which correlate well with accurate kinetic models. This allows to perform validation of various modeling approaches and analyze the basic physical mechanisms of the formation of the longitudinal spatial structure of the discharge ‘anatomy’.

In the implementation of the models described in section 2, the three plasma species, namely, electrons, positive ions, and metastable atoms were considered. Balance of charged particles is determined by the direct, stepwise, and Penning ionization processes. The set of plasma-chemical reactions is given in table 2, and collision cross-sections are shown in figure 2. Computed profiles of the discharge characteristics are demonstrated in figure 3. We have also included in this figure the results obtained from the fluid model with a nonlocal ionization source (see [8, 24] for details).

First, using the results of the kinetic model as a reference solution, let us list the main features of the ‘anatomy’ of the short discharge under consideration (see figure 3). The corresponding solution profiles were obtained using our in-house developed kinetic numerical code [36]. When analyzing and interpreting the results, we will also use scalings derived from analytical models [23, 24]. For the conditions under study, the length  $L$  of the discharge is less than the length of the inflection point  $L_{\text{inf}}$  on the Paschen curve. Therefore, the current–voltage characteristic (CVC) of this discharge is growing and no ballast resistance in the electric circuit is required to maintain it. The discharge is uniform over the cross-section and fills the entire surface of the cathode [23, 24]. Furthermore,

in a short discharge, the range of fast electrons with energies corresponding to the CF voltage is approximately equal to the discharge length  $L$  [23, 24]. In this case, fast electrons, accelerated in the strong field of the CF, excite and ionize the gas right up to the anode surface, so that the discharge consists exclusively of the NG, and the FDS and PC regions are not formed (figure 3).

The boundary of the cathode sheath occurs at the position of the highest glow intensity. The plasma density profile is close to parabolic with a maximum located approximately in the center of the plasma region [23, 24] (figure 3(d)). Near that point, the longitudinal electric field changes sign (figure 3(c)) to suppress electron diffusion toward the anode to ensure a constant current along the gas gap (for more details, see [23, 24]). The potential drop at the anode is negative (figures 3(b) and (c)), so that half of the ions produced in the plasma return back to the cathode, and the rest direct to the anode. In the longitudinal direction, the thermal electrons of the plasma are locked in a potential well in a weak electric field, so that their temperature is low ( $T_e < 1$  eV, figure 3(e)).

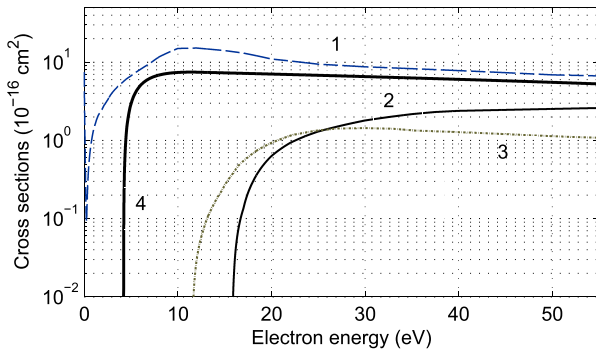
Due to invariance of the ambipolar diffusion equation for the plasma density with external ionization source in the product  $n_e T_e$  [24], error in  $T_e$  inevitably leads to error in  $n_e$ , i.e. overestimating  $T_e$  by several times leads to  $n_e$  being the same number of times underestimated. This fact can be clearly seen from figures 3(d) and (e) (see also [6, 47], where simulations were carried out with different values of  $T_e$ ).

The results presented in figure 3 clearly illustrate (see also [23, 24, 28]) inapplicability of LFA model in present situation. Indeed, the ionization rate derived from this model drops sharply (by several orders of magnitude compared to the results obtained from other models) in the region where the electric field is weak (figure 3(c)). As a result, the charged particles density obtained with LFA is distorted by several orders of magnitude compared to other methods (figure 3(d)). At the same time the LMEA model qualitatively reproduces the spatial distributions of discharge parameters, including such a subtle effect as reversing the sign of the electric field (figure 3(c)). However, significantly lower (more than an order of magnitude) absolute values of the plasma density are observed (figure 3(d)). The reason for this is an obvious overestimation of the electron temperature (figure 3(e)), and resulting underestimation of the density due to the invariant  $n_e T_e$ . Indeed, as can be seen from figure 3(e), the electron temperature obtained from the LMEA, which is a few eV, is about an order of magnitude higher than the temperature obtained from the kinetic model, which is about a fraction of an eV. Correspondingly, as can be seen from figure 3(d), the electron density  $n_e$  (and thus the ion density  $n_i$ ) provided by LMEA is underestimated by approximately an order of magnitude.

The reason for large errors in determining the electron density and temperature is due to the fact that in the LMEA model, as in any fluid model, the characteristics of the electron gas are determined by three main parameters (density, directional speed and temperature), which are found from the corresponding balance equations (3), (4), (6) and (7). Therefore, in the LMEA model, when deriving fluid equations, forced

**Table 2.** Elementary reactions considered in this study. Label Boltz. indicates that constant was calculated from local Boltzmann equation.

Index	Reaction	Type	$\Delta E$ (eV)	Rate constant
1	$e + Ar \rightarrow e + Ar$	Elastic collision	0	Boltz.
2	$e + Ar \rightarrow 2e + Ar^+$	Direct ionization	15.8	Boltz.
3	$e + Ar \leftrightarrow e + Ar^*$	Excitation	11.4	Boltz.
4	$e + Ar^* \rightarrow 2e + Ar^+$	Stepwise ionization	4.4	Boltz.
5	$2Ar^* \rightarrow e + Ar^+ + Ar$	Penning ionization	—	$6.2 \times 10^{-10} \text{ cm}^3 \text{ s}^{-1}$
6	$Ar^* \rightarrow h\nu + Ar$	Radiation (including trapping)	—	$1.0 \times 10^7 \text{ s}^{-1}$


**Figure 2.** Electron cross sections for (1) elastic, (2) direct ionization, (3) excitation, and (4) stepwise ionization collisions in argon, used in the model. Curve labels correspond to indices of corresponding processes in table 1.

factorization of the EEDF of the entire ensemble of electrons in the form of a product (2) is inevitably used. In approximation, ionization, which ensures the balance of charges, is determined exclusively by the plasma electrons themselves. Since maintaining a low-pressure discharge requires a sufficiently high level of charge production, the LMEA model inevitably overestimates the electron temperature to provide the required ionization level in the plasma of NG. The corresponding electron temperature is about several eV, as can be seen from figure 1.

In reality, ionization in plasma of NG is produced mainly due to fast ‘external’ electrons that have gained their energy outside the plasma, in the cathode sheath. These electrons behave independently of plasma electrons, so their characteristics do not depend on the behavior of plasma electrons as well as of plasma parameters of NG, the region which exhibits a weak (end even reversed, see figure 3(c)) electric field (for more details, see [23, 24, 48]). The actual temperature of plasma electrons is low, of the order of fractions of eV (see figure 3(f)), and these electrons do not contribute to the charge production. Therefore, in plasma of NG, any version of the fluid model *a priori* ignores the main channel of charge creation, namely, nonlocal ionization by fast electrons from the cathode layer. As a result, the LMEA model produces incorrect values of the main parameters of the NG plasma. This is a situation that cannot be resolved within the framework of any fluid model.

Apparent contradictions emerge from the basic postulate of LMEA, namely, a one-to-one correspondence between the electric field and the electron temperature, which underlies

the LMEA model. Indeed, when comparing the electric field obtained from this model with the ‘electric field’ calculated from the relationship in figure 1 from the electron temperature, as well as when comparing the ‘electron temperature’ obtained from the relationship in figure 1 from the electric field, strong discrepancies are observed (see figures 3(c) and (e)). Moreover, in a region with a reverse electric field, which cools rather than heats the electrons, a logically intractable situation arises regarding a relatively high electron temperature.

Considering all of the above, the irremovable inadequacy of the LMEA model is obvious even for the case of the simplest one-dimensional GD containing only one NG plasma region. In real situation, GDs have more complex spatial structure and consist of luminous NG and PC and dark FDS regions. Since PC can only exist in a geometry bounded in the transverse direction, modeling the entire GD requires solving the problem at least in a two-dimensional formulation; the relevant results and analysis are presented below.

### 3.2. 2D example

To explore the performance of LMEA in more detail, we performed 2D simulations of a long GD involving FDS and PC regions. More specifically, we carried out calculation for a discharge in argon, using the template for an axially symmetric 2D DC discharge, provided by the Plasma module of COMSOL Multiphysics [29]. In this model, plasma composition and plasma chemistry were specified identical to those in 1D model discussed in previous section (see table 2).

The axial and radial profiles of the discharge parameters are shown in figures 4 and 5. At first glance, the LMEA model reproduces all the basic regions of the GD (CF, NG, FDS, PC, and AF). Immediately behind the cathode layer, at the maximum density of the NG plasma, as in the previous example for the case of a short discharge, the longitudinal electric field changes sign. In contrast to a short discharge, in a long discharge, upon transition to a PC with a direct field, a second point of field reversal inevitably arises at the minimum plasma density. This phenomenon is clearly visible in figures 4(b) and 5(a). Further towards the anode there is a long PC with a constant plasma density along its length. In the present situation, the anode fall is positive, it attracts electrons and repels ions (although a case of a negative anode fall is also possible behind the PC). Therefore, in the immediate vicinity of the anode, the field increases sharply to ensure the required rate of ion production in a quasi-neutral plasma.

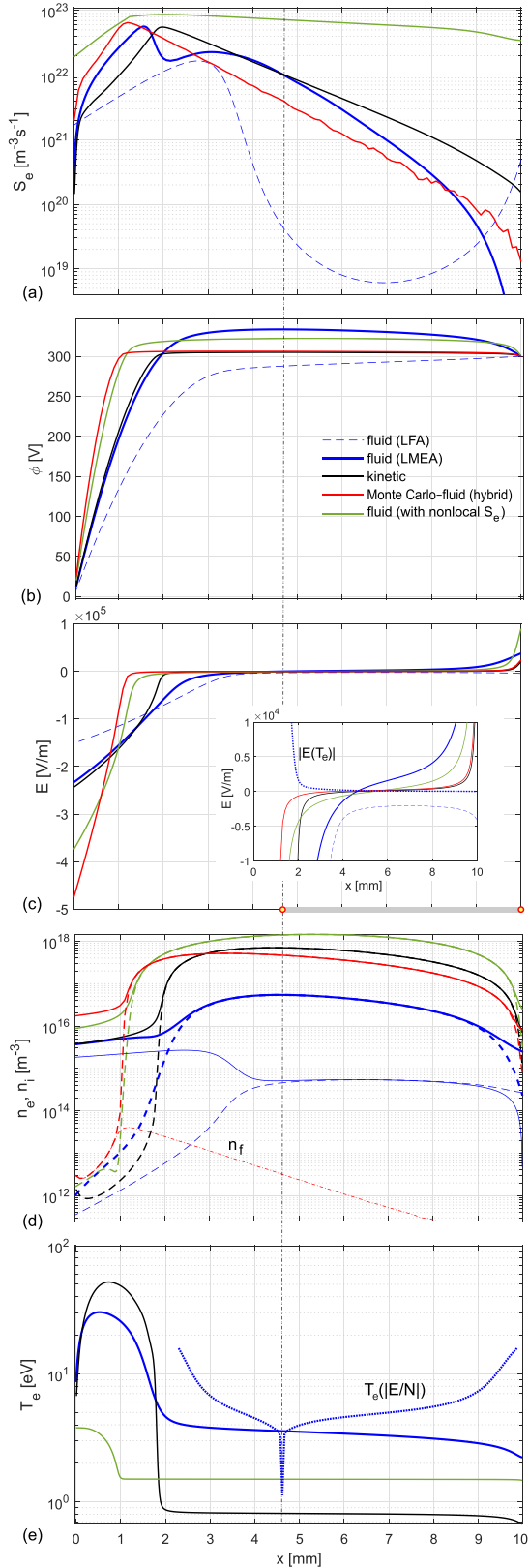


**Figure 3.** Spatial distributions of the (a) ionization source function, (b) electric potential, (c) electric field, (d) electron and ion number densities, and (e) electron temperature, computed from 1D models.  $n_f$  in (d) is fast electron density from MC-fluid (hybrid) model. Argon at pressure  $p = 1$  Torr, between electrode voltage  $U_d = 300$  V, gas gap width  $L = 1$  cm, secondary electron emission coefficient  $\gamma = 0.05$ . The legend shown in (b) applies to all panels. Small panel in (c) illustrates enlarged view of the field reversal.

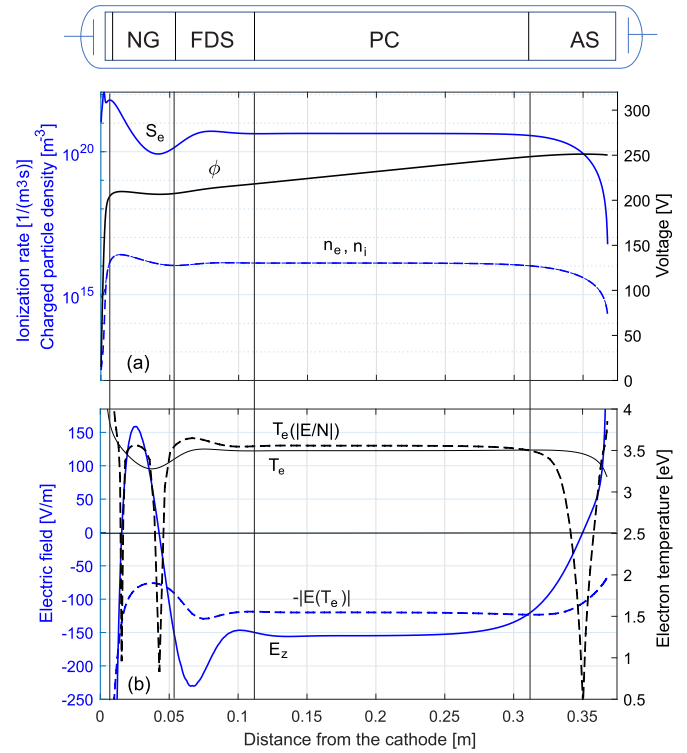


**Figure 4.** Axial profiles of the (a) ionization source function  $S_e$ , electric potential  $\phi$ , and electron and ion number densities  $n_e$  and  $n_i$ , (b) axial component of the electric field  $E_z$ , electron temperature  $T_e$ , and electric field  $E(T_e)$  and electron temperature  $T_e(|E/N|)$  obtained according to the correspondence through the electron Boltzmann equation depicted in figure 1. 2D (axially symmetric) model. Argon at pressure  $p = 0.5$  Torr, between electrode voltage  $U_d = 250$  V, gas gap width  $L = 37$  cm, radius of the discharge tube is  $R = 5$  cm, secondary electron emission coefficient  $\gamma = 0.1$ .

However, a closer look at all of these regions reveals the following inconsistencies.

Within the LMEA model, the thickness of the NG is specified by the shift between the spatial profiles of the electric field and electron temperature. This shift is estimated by the electron thermal conductivity length, which is  $\lambda_T = \lambda / \sqrt{2m_e/m_g} \approx 5$  cm, where the mean free path of electrons (for argon at a pressure of  $p = 0.5$  Torr) is defined as  $\lambda = 1/(N_0\sigma_M) \approx 0.025$  cm. This length, as can be seen from figures 4 and 5(a), corresponds to the width of the NG obtained from the LMEA model. However, according to experimental data in [49], at a pressure of 1 Torr for the potential fall of 250 V, the width of the NG is about 1 cm. The discrepancy arises due to the fact that the length of NG is determined by the range of fast electrons and is in no way related to the length of the electron thermal conductivity. This fact illustrates that the LMEA model is incapable of describing the parameters of NG plasma quantitatively.

Kinetic analysis also shows that both ionization and current transfer in NG are carried out by different groups of nonlocal electrons, which behave independently of each other and cannot be described by the integral characteristics (such as plasma density and temperature) of the entire ensemble of electrons as a whole (for details, see [23, 24]).



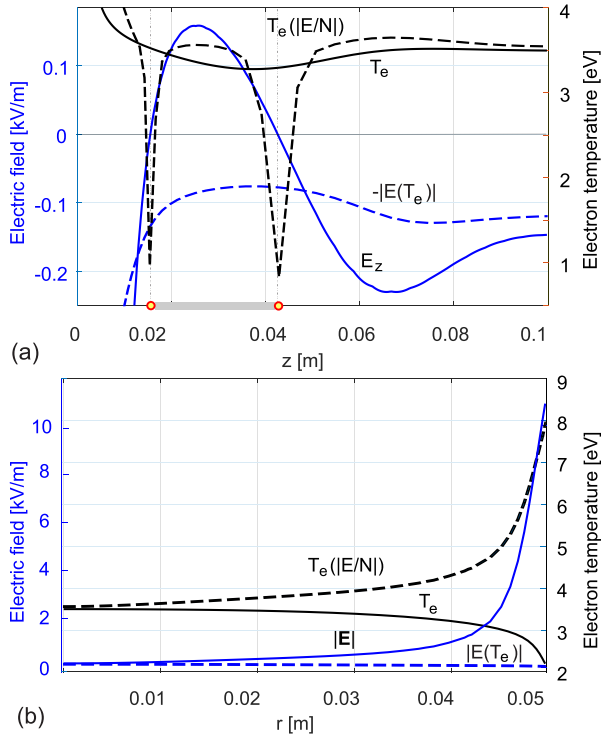


**Figure 5.** (a) Closer view to near cathode region from figure 4(b); (b) Radial profiles (through the positive column, at  $z = 0.2$  m) of the electric field  $|E|$ , electron temperature  $T_e$ , and electric field  $E(T_e)$  and electron temperature  $T_e(|E/N|)$  obtained according to the correspondence through the electron Boltzmann equation depicted in figure 1. All conditions are identical to those from figure 4.

As already mentioned in the introduction, perhaps the most paradoxical aspect in the longitudinal structure of the GD is occurrence of dark FDS region between two luminous NG and PC regions. This phenomenon cannot be explained within the framework of LFA for a conducting plasma with a constant current density in each discharge cross section. At first glance, figure 4 shows a dip in the electron density and temperature in the transition from NG to PC. In fact, the FDS is not reproduced within the LMEA. What is indicated as FDS in figure 4 is a kind of transition region between the NG and the PC. Indeed, the calculated electron temperature  $T_e$  in this region turns out to be greater than 3 eV (figure 4(b)), which implies that electron-induced excitation processes occur there. Consequently, the plasma in this region will actually not be ‘dark’, but ‘glowing’, which is in clear contradiction with the experimentally observed self-organization (‘anatomy’) of a GD.

As can be seen from figure 4, the main part of the long discharge is occupied by its PC. This is the most well known and studied plasma object. In particular, for the conditions under study, when the death of charges is determined by their ambipolar diffusion, the stationarity is provided by the Schottky condition

$$\nu_i = 1/\tau_{\text{amb}}. \quad (8)$$

Here, the characteristic time of ambipolar diffusion  $\tau_{\text{amb}} = R^2 / (2.4^2 \mu_i T_e)$  is determined by the geometry of the discharge volume and weakly depends on the electron temperature  $T_e$ . In turn, the ionization frequency  $\nu_i$  depends sharply on the electron temperature and is well approximated by Arrhenius formula  $\nu_i \sim \exp(-\varepsilon_i/T_e)$ . This frequency depends on the exponent with a large negative argument, so that using any EEDF sharply (exponentially) dependent on energy gives more or less similar values of the effective ‘temperatures’ of the fast part of the EEDF (for details, see [50]). This fact provides the reason for the possible agreement of some basic plasma parameters obtained using different, even very advanced modeling approaches, such as LMEA.

More detailed analysis carried out to date shows that in the PC at low and medium pressures the EEDF is nonlocal. This leads to a number of kinetic phenomena and effects that cannot be described in the traditional local approximation (see., e.g. [31, 50–53]). Therefore, any fluid modeling of plasma with nonlocal EEDF is, strictly speaking, incorrect, and the interpretation of the results obtained for such a plasma using any variation of fluid model should be treated with great caution.

Let us turn to the analysis of the main postulate of the LMEA model about the one-to-one correspondence between the electric field and the electron temperature through the electron Boltzmann equation (depicted in figure 1). For these purpose, in figures 3 and 4, in addition to the electron temperature profiles  $T_e$  calculated from the LMEA model, we included profile of  $T_e(|E/N|)$  obtained through the correspondence in figure 1, by using axial profile of the electric field  $E$ . Moreover, we included in these figures profiles of the electric field magnitude  $E(T_e)$ , obtained from the LMEA model, as well as recalculated through the dependence on the electron temperature  $T_e$  shown in figure 1.

Along the PC, as can be seen from figure 4(b), the profile of the electron temperature  $T_e$  agrees satisfactory with the profile of  $T_e(|E/N|)$  recalculated from the electric field. This is due to the fact that in the uniform longitudinal direction of the PC, the local value of the electron temperature is determined by the Joule heating in a uniform axial electric field. Thus, for the PC, when considering the longitudinal direction, the conditions for the applicability of the fluid model and, accordingly, the postulate of the LMEA model about the one-to-one correspondence of the electric field and temperature are approximately satisfied. However, in the transverse direction, where the plasma is inhomogeneous, the electron temperature is also variable. Figure 5(b) shows profiles of the electron temperature and electric field in the radial direction in the PC of the discharge, through the point  $z = 0.2$  m. In this situation, the discrepancy between  $T_e$  and  $T_e(|E/N|)$  is not only quantitative, but also qualitative.

The most obvious discrepancies between the profiles of  $T_e$  and  $T_e(|E/N|)$  are found in the near cathode plasma of the NG. As can be observed from figure 5(a), not only large quantitative but also qualitative differences are observed there. It can be seen that the electron temperature  $T_e(|E/N|)$ , recalculated from the electric field, is low in the region of weak electric field (and even tends to zero at points indicated in 5(a), where the

electric field goes to zero). It would seem that the ionization rate would be low here. However, the temperature  $T_e$ , obtained from the LMEA modeling (see figure 5(a)), takes on values that provide a fairly high level of ionization. Such different conclusions within the same model show that this approach is internally contradictory. Finally, within the framework of the LMEA model, the question remains unresolved as how to interpret the application of LMEA model to calculate the electron temperature in a reverse electric field (this region is indicated in 5(a)), which cools rather than heats the electrons.

Therefore, there is a fundamental disagreement and self-contradiction within this generally accepted and widely used model, which we address to the ‘computational plasma’ community.

#### 4. Conclusions

The work analyzes one of the most well-known modifications of the fluid model for GDs, which is sometimes referred to as the ‘extended fluid model’ or the ‘local mean energy approximation’ (LMEA). Its popularity is largely due to the fact that this model is implemented in the Plasma Module of the popular COMSOL Multiphysics computational package, which is widely used in practice for simulating various gas discharges in a wide range of conditions.

However, in the LMEA model, as in any other type of fluid model, the derivation of the basic equations is based on the assumption that the EEDF is local at a given point in space. This condition is satisfied only when the scale of plasma inhomogeneity is small compared to the electron energy relaxation length. A clear typical example when this is not true is the near cathode plasma of NG of discharges with flat and hollow cathodes, plasma of CCP discharges, and other short (without a positive column) discharges, in which ionization is carried out not by ‘local’ plasma electrons, but by ‘external’ electrons that gain their large kinetic energy from the outside, from space charge layers with a high electric field. In this context, careful and systematic model verification and validation in these situations is especially important.

The inconsistencies in the concept of LMEA are identified and illustrated by numerical examples. Within this model, the ability to obtain qualitatively plausible results in an inhomogeneous plasma is achieved by the following trick. First, through the relevant electron Boltzmann equation, a one-to-one correspondence is postulated between the electric field and the electron temperature, which actually occurs only under the conditions of applicability of fluid modeling. Further, finding the electron temperature from the electron energy balance, which takes into account the spatial transfer of heat due to thermal conductivity, without discussing the criteria of applicability, constants of volumetric processes of electron induced excitation, ionization, etc are determined as functions of the electron temperature, according to the accepted postulate. The apparent reliability of some basic discharge parameters calculated using this model, in our opinion, is unlikely to contribute to progress in modeling of gas discharge plasma. Moreover, the criteria and limits of applicability of the LMEA model are

not explicitly formulated, leaving this issue to the discretion of the individual researcher.


#### Data availability statement

All data that support the findings of this study are included within the article (and any supplementary files).

#### Acknowledgments

This work was supported by the National Key R&D Program of China (No. 2022YFE0204100), the Fundamental Research Funds for the Central Universities (No. HIT.OCEF.2022036) and the National Natural Science Foundation of China (No. 12375199).

#### ORCID iDs

Chen Zhou  <https://orcid.org/0000-0002-1361-3717>  
 Ismail Rafatov  <https://orcid.org/0000-0002-8303-9204>  
 Chengxun Yuan  <https://orcid.org/0000-0002-2308-6703>

#### References

- [1] Van Dijk J, Kroesen G and Bogaerts A 2009 *J. Phys. D: Appl. Phys.* **42** 190301
- [2] Donkó Z 2011 *Plasma Sources Sci. Technol.* **20** 024001
- [3] Alves L and Marques L 2012 *Plasma Phys. Control. Fusion* **54** 124012
- [4] Rafatov I, Bogdanov E and Kudryavtsev A 2012 *Phys. Plasmas* **19** 033502
- [5] Verboncoeur J P 2005 *Plasma Phys. Control. Fusion* **47** A231
- [6] Donkó Z, Hartmann P and Kutasi K 2006 *Plasma Sources Sci. Technol.* **15** 178
- [7] Derzsi A, Hartmann P, Korolov I, Karacsony J, Bánó G and Donkó Z 2009 *J. Phys. D: Appl. Phys.* **42** 225204
- [8] Rafatov I, Bogdanov E and Kudryavtsev A 2012 *Phys. Plasmas* **19** 093503
- [9] Hagelaar G and Pitchford L C 2005 *Plasma Sources Sci. Technol.* **14** 722
- [10] Kim H, Iza F, Yang S, Radmilović-Radjenović M and Lee J 2005 *J. Phys. D: Appl. Phys.* **38** R283
- [11] White R D, Robson R, Dujko S, Nicoletopoulos P and Li B 2009 *J. Phys. D: Appl. Phys.* **42** 194001
- [12] Robson R, White R D and Petrović Z L 2005 *Rev. Mod. Phys.* **77** 1303
- [13] Turner M M, Derzsi A, Donko Z, Eremin D, Kelly S J, Laffleur T and Mussenbrock T 2013 *Phys. Plasmas* **20** 013507
- [14] Arslanbekov R and Kolobov V 2018 Adaptive kinetic-fluid models for expanding plasmas *J. Phys.: Conf. Ser.* **1031** 012018
- [15] Tejero-del Caz A, Guerra V, Gonçalves D, Da Silva M L, Marques L, Pinhao N, Pintassilgo C and Alves L 2019 *Plasma Sources Sci. Technol.* **28** 043001
- [16] Fierro A, Barnat E, Moore C, Hopkins M and Clem P 2019 *Plasma Sources Sci. Technol.* **28** 055012
- [17] Alves L, Bogaerts A, Guerra V and Turner M 2018 *Plasma Sources Sci. Technol.* **27** 023002
- [18] Stankov M, Becker M M, Hoder T and Loffhagen D 2022 *Plasma Sources Sci. Technol.* **31** 125002
- [19] Colonna G and D’Angola A 2022 *Plasma Modeling: Methods and Applications* (IOP Publishing)

- [20] Dujko S, Markosyan A, White R and Ebert U 2013 *J. Phys. D: Appl. Phys.* **46** 475202
- [21] Becker M M, Kählert H, Sun A, Bonitz M and Loffhagen D 2017 *Plasma Sources Sci. Technol.* **26** 044001
- [22] Alvarez Laguna A, Esteves B, Bourdon A and Chabert P 2022 *Phys. Plasmas* **29** 083507
- [23] Kolobov V and Tsendin L 1992 *Phys. Rev. A* **46** 7837
- [24] Kudryavtsev A, Morin A and Tsendin L 2008 *Tech. Phys.* **53** 1029–40
- [25] Kudryavtsev A and Tsendin L 2001 *Tech. Phys. Lett.* **27** 284–8
- [26] Yuan C, Kudryavtsev A A and Demidov V I 2018 *Introduction to the Kinetics of Glow Discharges* (Morgan & Claypool Publishers)
- [27] Boeuf J and Pitchford L 1995 *Phys. Rev. E* **51** 1376
- [28] Grubert G, Becker M and Loffhagen D 2009 *Phys. Rev. E* **80** 036405
- [29] COMSOL MULTIPHYSICS v. 6.1 2022 Plasma Module user's guide Stockholm (COMSOL AB) (available at: [www.comsol.com](http://www.comsol.com))
- [30] CFD-ACE+ v. 2014.0 Modules manual Huntsville (ESI Group) (available at: [www.esi-group.com/](http://www.esi-group.com/))
- [31] Tsendin L, Bogdanov E and Kudryavtsev A 2005 *Phys. Rev. Lett.* **94** 015001
- [32] Yuan C, Bogdanov E, Kudryavtsev A, Rabadanov K and Zhou Z 2017 *Sci. Rep.* **7** 14613
- [33] Raizer Yu P 2011 *Gas Discharge Physics* (Springer)
- [34] Hagelaar G, De Hoog F and Kroesen G 2000 *Phys. Rev. E* **62** 1452
- [35] Winkler R, Arndt S, Loffhagen D, Sigenefer F and Uhrlandt D 2004 *Contrib. Plasma Phys.* **44** 437–49
- [36] Yuan C, Bogdanov E, Eliseev S and Kudryavtsev A 2017 *Phys. Plasmas* **24** 073507
- [37] Kolobov V I and Arslanbekov R R 2006 *IEEE Trans. Plasma Sci.* **34** 895–909
- [38] Birdsall C K 1991 *IEEE Trans. Plasma Sci.* **19** 65–85
- [39] Vahedi V and Surendra M 1995 *Comput. Phys. Commun.* **87** 179–98
- [40] Kawamura E, Birdsall C K and Vahedi V 2000 *Plasma Sources Sci. Technol.* **9** 413
- [41] Erden E and Rafatov I 2014 *Contrib. Plasma Phys.* **54** 626–34
- [42] Arda I and Rafatov I 2023 *Turk. J. Phys.* **47** 198–213
- [43] Surendra M, Graves D and Jellum G 1990 *Phys. Rev. A* **41** 1112
- [44] Fiala A, Pitchford L and Boeuf J 1994 *Phys. Rev. E* **49** 5607
- [45] Bogaerts A, Gijbels R and Goedheer W 1995 *J. Appl. Phys.* **78** 2233–41
- [46] Kushner M J 2009 *J. Phys. D: Appl. Phys.* **42** 194013
- [47] Eylenceoğlu E, Rafatov I and Kudryavtsev A 2015 *Phys. Plasmas* **22** 013509
- [48] Rozhansky V A and Tsendin L D 2001 *Transport Phenomena in Partially Ionized Plasma* (CRC Press)
- [49] Brewer A K and Westhaver J 1937 *J. Appl. Phys.* **8** 779–82
- [50] Bogdanov E, Kudryavtsev A, Tsendin L, Arslanbekov R, Kolobov V and Kudryavtsev V 2003 *Tech. Phys.* **48** 983–94
- [51] Bogdanov E, Kudryavtsev A, Tsendin L, Arslanbekov R, Kolobov V and Kudryavtsev V 2003 *Tech. Phys.* **48** 1151–8
- [52] Bogdanov E, Kudryavtsev A, Tsendin L, Arslanbekov R, Kolobov V and Kudryavtsev V 2004 *Tech. Phys.* **49** 698–706
- [53] Bogdanov E, Kudryavtsev A, Tsendin L, Arslanbekov R and Kolobov V 2004 *Tech. Phys.* **49** 849–57